

Observation of kink instability during small B5.0 solar flare on 04 June, 2007

A.K. Srivastava¹

aks@aries.res.in

T.V. Zaqarashvili^{2,3}

teimuraz.zaqarashvili@oeaw.ac.at

Pankaj Kumar¹

pkumar@aries.res.in

and

M.L. Khodachenko²

maxim.khodachenko@oeaw.ac.at

Received _____; accepted _____

¹Aryabhata Research Institute of Observational Sciences (ARIES), Nainital-263129, India

²Space Research Institute, Austrian Academy of Sciences, Graz 8042, Austria

³Abastumani Astrophysical Observatory at Ilia State University, Al Kazbegi ave. 2a, 0160 Tbilisi, Georgia

ABSTRACT

Using multi-wavelength observations of SoHO/MDI, SOT-Hinode/blue-continuum (4504 Å), G-band (4305 Å), Ca II H (3968 Å) and TRACE 171 Å, we present the observational signature of highly twisted magnetic loop in AR 10960 during the period 04:43 UT–04:52 UT at 4 June, 2007. SOT-Hinode/blue-continuum (4504 Å) observations show that penumbral filaments of positive polarity sunspot have counter-clock wise twist, which may be caused by the clockwise rotation of the spot umbrae. The coronal loop, whose one footpoint is anchored in this sunspot, shows strong right-handed twist in chromospheric SOT-Hinode/Ca II H (3968 Å) and coronal TRACE 171 Å images. The length and the radius of the loop are $L \sim 80$ Mm and $a \sim 4.0$ Mm respectively. The distance between neighboring turns of magnetic field lines (i.e. pitch) is estimated as ≈ 10 Mm. The total twist angle, $\Phi \sim 12\pi$ (estimated for the homogeneous distribution of the twist along the loop), is much larger than the Kruskal -Shafranov instability criterion. We detected clear double structure of the loop top during 04:47–04:51 UT on TRACE 171 Å images, which is consistent with simulated kink instability in curved coronal loops (Török et al. 2004). We suggest, that the kink instability of this twisted magnetic loop triggered B5.0 class solar flare, which occurred between 04:40 UT and 04:51 UT in this active region.

Subject headings: sunspots — sun: magnetic fields — sun: flares — sun: chromosphere — sun: corona

1. Introduction

Solar coronal magnetic field has complex topology which is caused due to photospheric motions and emergence of new magnetic flux. The complex configurations often lead to various instability processes, which eventually trigger solar flares and CMEs (Coronal Mass Ejections). Kink instability is one of those processes and it is connected to the azimuthal twist of magnetic tubes. The exact amount of twist required to trigger the kink instability depends on various factors including loop geometry and overlying magnetic fields (e.g., Hood and Priest, 1979; Lionello et al., 1998; Baty et al., 1998; Baty, 2001; Török et al., 2004; Fan and Gibson, 2003, 2004, Leka et al., 2005 and references therein). Recent observations of kink instability accompanied with full filament eruption (Williams et al., 2005), partial cavity eruption (Liu et al., 2007), partial filament eruption (Liu et al. 2008), and failed filament eruption (Alexander et al. 2006) indicate to its importance in filament interaction with magnetic environment. Kink instability is also found to be an efficient mechanism for solar eruptive phenomena, e.g, triggering solar flares and CMEs (Sakurai 1976; Hood, 1992; Török and Kliem 2005; Kliem and Török, 2006 and references therein).

Although we have few observational evidences of kink instability in various magnetic structures (e.g., coronal loops, filaments), the theory is much more established in terms of modeling and numerical simulations. Previous theoretical models, based on straight tube assumption, have studied intensively various aspects of kink instability in the solar corona including the formation of current sheets (Baty and Heyvaerts 1996; Gerrard et al., 2001; Gerrard and Hood, 2003; Hynes and Arber 2007) and magnetic topology (Baty, 2000; Lionello et al., 1998). Later on, more sophisticated models based on curved flux tube geometry, addressed the formation of current sheets (e.g. Török et al., 2004), loop response to injected twist through its footpoints (e.g., Klimchuk, 2000; Tokman and Bellan, 2002; Aulanier et al., 2005 and references cited there), and eruption of kink unstable loops

through overlaying arcades (e.g. Török and Kliem, 2005; Fan, 2005).

In this paper, we present the observational evidence of highly twisted coronal loop in the AR NOAA 10960 as observed on 04 June, 2007 between 04:43 UT and 04:52 UT, which probably caused B5.0 class flare during this time. We use observations from several different instruments in order to cover almost whole solar atmosphere. SOHO/MDI and SOT-Hinode/blue-continuum (4504 Å) have been used to observe the photospheric part of the active region. We used data from SOT-Hinode Ca II H (3968 Å) to study the chromospheric level. Finally, TRACE 171 Å observations are used to study the coronal structure. In Section 2, we describe multi-wavelength observations of twist and kink instability in AR 10960 on 04 June, 2007. In Section 3, we present some theoretical interpretations. In the last section, we present some discussions and conclusions.

2. Multi-wavelength observations of kink instability in AR 10960

The active region NOAA 10960 has been observed by various spacecrafts on 04 June, 2007. The active region was located nearby the eastern limb of the southern hemisphere near the equatorial plane at S09E50 with $\beta\gamma\delta$ field configuration of the sunspot group. This active region produced ten M-class flares during its journey over the whole solar disk. However, this active region was poor CME originator, and only two from all M-class flares were associated with CMEs. The active region has produced a confined M8.9/3B flare on 04 June, 2007 without triggering CME. The flare has an impulsive rise phase for a short duration between 05:06 UT and 05:13 UT and a gradual decay for a long time nearly up to 06:45 UT. Kumar et al. (2009) have recently described a detailed multiwavelength view of this M8.9/3B class solar flare, and concluded that the positive flux emergence and the penumbral filaments loss of the associated sunspot and the activation of the several twisted flux ropes in and around the flare site, may be the key candidates for the occurrence of

this flare. However, a small B5.0 class flare has also been observed during 04:40-04:51 UT, which seems to be a precursor for the M8.9 flare. This B-class, small and confined flare was also evident in the GOES soft X-ray profile during 04:40 UT–04:51 UT of 04 June, 2007.

Below we explore the relation between this B-class small flare, which may have triggered the M-class flare later, and the magnetic structure of the active region. During the flaring time, we detected the strong helical twist in the coronal loop, which was associated to the flare. Figure 1 shows the coronal image of AR 10960 as observed from Transition Region and Coronal Explorer (TRACE) in 171 Å line on 04:48:55 UT at 04 June, 2007. The TRACE field of view is overlaid by co-aligned MDI (Michelson Doppler Imager) contours showing positive (white) and negative (black) magnetic polarities. One footpoint of the coronal loop is associated with a small positive magnetic polarity spot (above which the helical twist and simultaneous brightening has been observed during 04:43 UT and 04:52 UT). Another footpoint is probably anchored in a small leading spot with negative polarity in the same active region.

High-resolution filtergrams of NOAA 10960 at photospheric and chromospheric levels were obtained by 50 cm Solar Optical Telescope (SOT) onboard Hinode spacecraft at 04 June, 2007. We use the SOT/blue-continuum (4504 Å), G-band (4305 Å) photospheric and SOT/Ca II H (3968 Å) chromospheric image data at a cadence of ~ 1 minute, with a spatial resolution of 0.1'' per pixel (Tsuneta et al., 2008). The data are calibrated and analysed using standard routines in the SolarSoft (SSW) package.

Figure 2 displays the partial field of view of TRACE 171 Å image on 04:48:15 UT at 04 June 2007, which shows the coronal loop segment with activated helical twist. The TRACE temporal image data of 1 minute cadence is calibrated and also co-aligned using Solar-Soft routines. The co-aligned SOT G-band (left panel) and Ca II (right panel) contours are overlaid on TRACE 171 Å image. The G-band contour shows the position

of sunspot which probably is the source of helical twist, while the Ca II contour shows the chromospheric part of the loop segment. The solar loops associated with active regions of the southern hemisphere, usually show the predominant right-handed twist according to the Hemisphere Helicity Rule (HHR) (Tian et al., 2002, 2005 and references cited there). The coronal loop shown in the Figure 2 also exhibits a right-handed twist and thereby follows the HHR.

Figure 3 shows the time series of SOT/blue-continuum (4504 \AA) during 04:36 UT and 04:52 UT at an intervals of 4-5 min on 04 June, 2007 (lower panel). This small positive polarity spot, where the left footpoint of twisted coronal loop is anchored, is a small part of a big active region AR10960 (upper panel). The active region was associated with the descending phase of the solar cycle 23. It obeys both, the Hale-Nicholson Law (Hale and Nicholson, 1925) and the Joy’s Law (Hale et al., 1919). Bipolar active regions are believed to be formed due to rising of Ω -shaped magnetic flux tubes through the convection zone (Babcock, 1961, Zwaan, 1985). The axes of bipolar active regions are then tilted towards the equator due to the Coriolis force resulting in a counter-clockwise rotation in the southern hemisphere and vice-versa (e.g., Wang & Sheeley, 1989; Howard, 1991; Tian et al., 2001; 2002; 2003, 2005, Zhang & Tian 2005 and references therein). Numerical simulations also show that the newly emerged magnetic tubes are supposed to be twisted during the rising phase through the convection zone (Moreno-Insertis and Emonet 1996; Archontis et al. 2004). On the other hand, Sturrock & Woodbury (1967) proposed that the photospheric latitudinal differential rotation may lead to a clockwise (counterclockwise) rotation of sunspots about their axes in the southern (northern) hemisphere. Observed rotation of sunspots (Brown et al. 2003, Yan and Qu 2007) may lead to twist in and above active regions. The high-resolution morphology on Figure 3 shows that the penumbral filaments of the spot are highly twisted and sheared in the counter-clockwise direction. In order to be sure about the emergence of new magnetic flux during B5.0 flare in AR 10960

(04:40 UT–04:51 UT), the high cadence magnetograms (e.g., SOT/Hinode magnetograms) are needed. Unfortunately, the SOT magnetograms are unavailable for this period. We examined 96-min cadence SoHO/MDI magnetograms, available at 03:15 UT and 04:51 UT, and found no new flux emergence in and around the positive polarity sunspot. Therefore, under the observational limitations, it is most likely that the clock-wise rotation of the spot umbrae is responsible for the counter clock-wise twist of penumbral filaments. Indeed, some evidence of insignificant clock-wise rotation of the umbral part can be seen from 04:36 UT and later (see lower panel, Figure 3). The rotation is more pronounced in SOT/blue-continuum movie. Unfortunately, there are no observational data before the time, therefore we are not completely sure about the rotation and its rate.

Rotation and twisting of sunspots at the photospheric level eventually lead to the twisting of magnetic field lines in higher regions. Therefore, the rotation of the spot probably play a role in the generation of right-handed twist in associated coronal loop which is consistent with many previous findings (e.g. Bao et al. 2002; Brown et al. 2003, Tian et al. 2008 and references therein). Tian et al. (2008) have found the significant counter-clockwise rotation in the AR sunspots of northern hemisphere during the same solar cycle which generates the left-handed twist in the associated loop system. Figure 4 displays the time series of SOT/Ca II H (3968 Å) during 04:43 UT and 04:52 UT at 04 June 2007. The time series shows the clear twist just above the spot and consequent activation of the helical twist in the chromospheric part of the coronal loop during B5.0 class flare (i.e. between 04:40 UT–04:51 UT). The brightening of chromospheric plasma is also seen during the time interval, which may show the evidence of heating.

Helical twist is more clearly seen in the coronal part of AR 10960. Figure 5 shows the time series of TRACE 171 Å in the same active region and during the same time interval 04:43–04:52 UT. The plasma brightening during the B5 flare is clearly seen. The brightening

reveals clear helical twist of the coronal loop which connects two different polarities in the active region (see Figure 1). The writhe of the coronal loop is not clearly identified, therefore we can not say whether the loop has S- or reverse S-structure. However, the right-handed twist can be easily identified between 04:45 and 04:52 UT, especially in its left footpoint. Thus, the loop was strongly twisted during the B5.0 flare (04:40-04:51 UT). The loop footpoint is only seen during the brightening phase i.e. during 04:40 UT–04:51 UT, therefore we could not trace how the twist was formed. It seems that the loop was already twisted, but the brightening just made it observable.

Especially interesting event is observed during 04:47-04:51 UT on TRACE 171 Å images (Figure 5). It seems that the loop top is split into two parts and shows double structure during this time (the double structure is clearly seen on Figure 1 as well). We have also analyzed XRT/Hinode Ti-Poly temporal image data of the same active region. We use the standard methods to calibrate the data and correct the orbital variations to see the co-spatial X-ray brightening of the flare in this loop (Shimzu et al., 2007). Sudden brightening and enhancement of soft X-ray flux in the loop has also been observed around 04:49 UT by XRT/Hinode. Thus, the double structure of loop top in 171 Å coincides to the enhancement of soft X-ray flux.

Recently Török et al. (2004) performed numerical simulations of kink instability of twisted coronal loops and show that the kink perturbations with a rising loop apex lead to the formation of a current sheet below the apex, which does not occur in the cylindrical approximation. The double structure of coronal loop at its top is seen in the numerical simulations (see Figure 3 in Török et al. 2004), which is quiet similar to that we observe during 04:47-04:51 UT. Therefore, we find the most likely evidence of the kink instability in the twisted coronal loop, which triggers the small B5.0 class flare during 04:40 UT–04:51 UT.

In the next section we estimate the loop parameters, the value of twist and make some theoretical suggestions.

3. Theoretical estimations

Most clear image of twisted loop in TRACE 171 Å series is seen at 04:49:36 UT, therefore we use this frame for estimation of loop parameters.

The projected distance between loop footpoints is ~ 40 Mm. However, the real distance can be increased up to 50 Mm taking into account the projection effects. Using the ideal semi-torus form we may estimate the loop real length as

$$L = \pi R \approx 80 \text{ Mm}, \quad (1)$$

where R is the big radius of torus. The loop small radius at the middle of left side can be estimated as $a \approx 4$ Mm.

An important parameter of straight twisted tubes is

$$p = \frac{aB_z}{B_\phi}, \quad (2)$$

where B_z and B_ϕ are the longitudinal and azimuthal components of magnetic field, and $2\pi p$ is called as *pitch*. Then the pitch can be expressed by loop length and the number of turns over the tube length (N_{twist}) as

$$2\pi p = \frac{L}{N_{twist}}. \quad (3)$$

The total twist angle is then

$$\Phi = 2\pi N_{twist} = \frac{LB_\phi}{aB_z}. \quad (4)$$

At least, 3 different turns are seen along the left half length of the loop at 04:49:36 UT (see Fig. 5). The mean pitch, i.e. the distance between neighboring turns of magnetic field lines, is estimated as $2\pi p \approx 10$ Mm, while the total twist angle for the left half of the loop is roughly

$$\Phi \approx 6.0\pi. \quad (5)$$

The right footpoint is not seen clearly in the TRACE images, therefore we can not estimate the number of turns there. Some helicity imbalance may exist between the two ends of the loop (Tian and Alexander, 2009; Fan et al., 2009). This is also evident from the Hinode/SOT WB full FOV image (Figure 3), where the opposite polarity sunspots seem to have imbalanced morphology. However, this asymmetric helicity (if any) does not mean that the twist will be inhomogeneous along the loop. The initial asymmetric distribution of twist along the loop can be smoothed out over Alfvén time (Fan et al., 2009). Our observed loop with the length of 80 Mm and average coronal Alfvén speed of 1000 km s^{-1} implies the Alfvén time as $t = L/V_A \sim 80$ s. Thus, any asymmetry in the twist distribution will be smoothed out within ~ 80 s. In other words, the rotation of one footpoint may cause the twisting of whole loop, even if the spot, where the second footpoint is anchored, does not rotate. Therefore, we may consider the quasi-symmetric twist along the whole loop during 04:40 UT–04:51 UT when B5.0 flare was triggered. Then 3 more turns along the right half length of the loop are expected, which give the total twist angle for the whole loop as

$$\Phi \approx 12\pi. \quad (6)$$

This is a rather strong twist. However, even if we consider the lower bound of total twist angle, 6π (estimated from the left half part of the loop), the loop could be unstable to kink instability, which eventually may lead to observed B-class flare.

Kink instability is caused due to the growth of $m = 1$ mode, which displaces the tube axis. General properties of classical kink instability are well studied. Kruskal -Shafranov

instability criterion yields $\Phi > 2\pi$. Line tying of loop footpoints at the photospheric level generally increases the critical twist angle and the instability threshold becomes $\Phi > 2.5\pi$ (Hood and Priest 1979). However, for the large aspect ratio (i.e. the ratio between loop length and radius), the critical twist angle increases further (Baty 2001). The approximate aspect ratio of our loop is $L/a \approx 20$, which is quite large. Normal mode analysis in the thin tube approximation (i.e. for large aspect ratio) gives the instability criterion as $a > 2p$ (Dungey and Loughhead, 1956, Bennett et al. 1999), which yields also large twist angle. In our loop parameters, this gives the critical twist angle of $\Phi \approx 12\pi$, which is very close to the angle estimated from the homogeneous twist. Longitudinal flow along twisted magnetic tube may reduce the critical twist angle, thereby enhances the probability of the kink instability (Zaqarashvili et al. 2010). However, no clear evidence of flow is detected in our observations.

Numerical simulations of Török et al. (2004) have been performed for a curved loop taking into account the line-tying conditions. They used the twisted loop model of Titov and Demouline (1999) and show that the loop is subject to ideal kink instability. They estimated the critical twist angle for different parameters of coronal loops. Török et al. (2004) solved the case of $R/a = 5$ and showed that the critical twist angle is $\Phi_c \approx 3.5$ for $R=110,000$ Mm, although these parameters are much larger comparing to our loop. On the other hand, the critical twist angle probably increases for smaller a (Baty 2001). Unfortunately, Török et al. (2004) did not estimate a critical twist angle for loop parameters, which are close to our loop. However, general behaviour of the twisted loop could be similar to what they have shown in their paper. Namely, the double structure of loop top (Figure 3 of their paper) seems quite similar to what we have observed here (Figure 5).

4. Discussion and conclusions

Using multiwavelength observations of SoHO/MDI, SOT-Hinode/blue-continuum (4504 Å), G-band (4305 Å), Ca II H (3968 Å) and TRACE 171 Å, we find the observational signature of highly twisted coronal loop in AR 10960 during the period of 04:43 UT-04:52 UT at 04 June, 2007. This twisted loop was probably unstable to the kink instability, which triggered small B-class flare during the same time. SOT-Hinode/blue-continuum (4504 Å) images show that the penumbral filaments of small positive polarity sunspot have counter-clock wise twist around its center (Figure 3). The twist is probably caused by the clockwise rotation of the sunspot umbrae as expected in the southern hemisphere. The observed coronal loop whose one footpoint is anchored in this spot, shows strong right-handed twist in chromospheric (Ca II H 3968 Å , Figure 4) and coronal (TRACE 171 Å , Figure 5) images. We estimated the loop length and radius as ~ 80 and ~ 4 Mm respectively. From TRACE 171 Å time sequence we estimate the pitch of twisted loop as ~ 10 Mm. The twist is assumed to be homogeneous along the whole loop as any asymmetry can be quickly smoothed out over the Alfvénic time, which is estimated as ~ 80 s for our loop. The total twist angle for the whole loop is $\Phi \sim 12\pi$ in the case of homogeneous distribution. This is much larger than the Kruskal-Shafranov kink instability criterion, and approximately equal to the more conservative thin-tube estimate for the kink instability. The loop top shows clear double structure during 04:47-04:51 UT, which was accompanied by sudden enhancement of soft X-ray flux around 04:49 UT observed by XRT/Hinode.

The strong twist of the coronal loop probably leads to the kink instability, although no clear displacement of the loop axis or sigmoid structure have been detected during the flaring time. However, the observed double structure of the loop top probably indicates to the current sheet induced by the kink instability as it was suggested by numerical simulations (Török et al. 2004). This current sheet probably triggered the B-class flare via

reconnection.

Instability of internal kink mode (Arber et al. 1999; Haynes and Arber, 2007), where the kink structure is not apparent from the global field shape of the active region, may be considered as a triggering mechanism for the B-class flare. Haynes and Arber (2007) considered the example of short coronal loop ($L= 10$ Mm) with zero net current. This means that the magnetic twist changes the sign along the loop radius, which causes the confinement of unstable kink mode in space. This process has also been shown by Arber et al. (1999) to release sufficient energy to cause a transient brightening of confined loops. However, there are some questions related to the simulation of Haynes and Arber (2007). First, our observed loop is longer compared with the simulated one by a factor of 8. Therefore, it is unclear if the same mechanism may work for longer loops. Second, it is unclear why the twist should have opposite signs along the tube radius. Haynes and Arber (2007) considered photospheric motion as a generator of this configuration, however no clear process has been suggested.

Twisted coronal loops can be also subject to the sausage instability. Linear sausage pinch instability occurs when $B_\phi^2 > 2B_z^2$ (Aschwanden 2004). It gives the critical twist angle of $\sim 9\pi$ in our loop parameters. Nonlinear analysis of Zaqarashvili et al. (1997) shows even smaller critical twist angle. The observed twist in our loop is much larger. However, the sausage pinch does not lead to observed double structure at the loop top, which rules out the occurrence of sausage instability in the loop.

It is quiet possible that the observed twist of coronal loop corresponds to the helical structure formed after the kink instability. Then, the radius of the loop will be bit smaller than ~ 4 Mm. However, this means that the wave length of unstable mode is ~ 15 Mm (i.e. twice the distance between neighboring bright areas along the loop, see Figure 5), which is much less comparing to the loop length. It means that the higher order harmonic rather

than fundamental one was unstable to the kink instability. This unexpected fact needs special justification, which may require detailed numerical simulations.

It should be mentioned, that the small B5.0 flare was precursor for stronger M-class flare, which occurred just 15 min later at 05:06 UT. It is possible that the magnetic field reconfiguration due to the small B5.0 flare caused global kink instability with consequent reconnection and global energy release. It is interesting to check whether the big flares are usually preceded with smaller energy release. Liu et al. (2003) and Gary and Moore (2004) have observed recurrent flare activity of the active region AR 10030 in the northern hemisphere on 15 July 2002, which was accompanied by CME. The large flare/CME was preceded by a small flare and the authors supposed the rise of helical flux rope as the source for the activity. Their observations show strongly twisted loop in TRACE images (see Fig. 1 in Gary and Moore, 2004), which arose upwards and disappeared during short time interval (~ 50 s). One may suggest that the strong twist of our loop may be also formed due to the similar rise of magnetic flux rope. However, there are significant differences between the observations. First, no new magnetic flux emergence is seen at the photospheric level in our case. And second, our twisted loop stays unchanged during longer time interval (at least 5 min) and no sign of upward motion is detected. Therefore, we think that the rise of helical flux rope is not relevant to our observations, which probably suggests at least two different triggering mechanisms for solar flares. The similarity between the two events is that the small flares seem to be the pre-cursors of large flares. On the other hand, the flare in the active region AR 10030 on 15 July 2002 was accompanied by CME (Liu et al. 2003, Gary and Moore 2004), while the flare in AR 10960 on 04 June 2007 was not (Kumar et al., 2010). Therefore, we suggest that the large flares accompanied with energetic CMEs can be triggered by flux-rope eruption with significant changes in the photospheric fields, while the moderate flares without CME are triggered by some instabilities (e.g., kink instability). More statistical study is required to make a firm conclusion.

In conclusion, we observe the strong twist of coronal loop in AR 10960 during small B5.0 flare between 04:43 UT–04:52 UT at 04 June, 2007. The loop top shows clear double structure, which is consistent with simulated kink instability of curved coronal loop (Török et al. 2004). We suggest that the current sheet formed at the loop top due to the kink instability was the reason for the B5.0 flare.

This work is supported by the grant of a joint Indo-Russian (INT/RFBR/P-38) DST-RFBR project, the Austrian Fond zur Förderung der Wissenschaftlichen Forschung (project P21197-N16) and the Georgian National Science Foundation grant GNSF/ST09/4-310. Hinode is a Japanese mission developed and launched by ISAS/JAXA, with NAOJ as domestic partner and NASA and STFC (UK) as international partners. It is operated by these agencies in co-operation with ESA and NSC (Norway). We also acknowledge MDI/SoHO and TRACE observations used in this study. We thank the anonymous referee for constructive suggestions which improved the manuscript considerably.

REFERENCES

- Alexander, D., Liu, R., & Gilbert, H. R. 2006, *ApJ*, 653, 719
- Archontis, V., Moreno-Insertis, F., Galsgaard, K., Hood, A., & O’Shea, E. 2004, *A&A*, 426, 1047
- Aschwanden, M.J., 2004, *Physics of the Solar Corona*, Springer.
- Arber, T. D., Longbottom, A. W., & van der Linden, R. A. M. 1999, *ApJ*, 517, 990
- Aulanier, G., Démoulin, P., & Grappin, R. 2005, *A&A*, 430, 1067
- Babcock, H. W. 1961, *ApJ*, 133, 572
- Bao, S. D., Sakurai, T., & Suematsu, Y. 2002, *ApJ*, 573, 445
- Baty, H., & Heyvaerts, J. 1996, *A&A*, 308, 935
- Baty, H., Einaudi, G., Lionello, R., & Velli, M. 1998, *A&A*, 333, 313
- Baty, H. 2000, *A&A*, 360, 345
- Baty, H. 2001, *A&A*, 367, 321
- Bennett, K., Roberts, B., & Narain, U. 1999, *Sol. Phys.*, 185, 41
- Brown, D. S., Nightingale, R. W., Alexander, D., Schrijver, C. J., Metcalf, T. R., Shine, R. A., Title, A. M., & Wolfson, C. J. 2003, *Sol. Phys.*, 216, 79
- Dungey, J. W., & Loughhead, R. E. 1954, *Australian Journal of Physics*, 7, 5
- Fan, Y., & Gibson, S. E. 2003, *ApJ*, 589, L105
- Fan, Y., & Gibson, S. E. 2004, *ApJ*, 609, 1123

- Fan, Y. 2005, ApJ, 630, 543
- Fan, Y., Alexander, D., & Tian, L. 2009, ApJ, 707, 604
- Gary, G.A., & Moore, R.L. 2004, ApJ, 611, 545
- Gerrard, C. L., Arber, T. D., Hood, A. W., & Van der Linden, R. A. M. 2001, A&A, 373, 1089
- Gerrard, C. L., & Hood, A. W. 2003, Sol. Phys., 214, 151
- Hale, G. E., Ellerman, F., Nicholson, S. B., & Joy, A. H. 1919, ApJ, 49, 153
- Hale, G. E., & Nicholson, S. B. 1925, ApJ, 62, 270
- Haynes, M., & Arber, T. D. 2007, A&A, 467, 327
- Hood, A. W., & Priest, E. R. 1979, Sol. Phys., 64, 303
- Hood, A. W. 1992, Plasma Physics and Controlled Fusion, 34, 411
- Howard, R. F. 1991, Sol. Phys., 136, 251
- Kliem, B., Török, T. 2006, Physical Review Letters, 96, 255002
- Klimchuk, J. A. 2000, Sol. Phys., 193, 53
- Kumar, P., Srivastava, A. K., Filippov, B., Uddin, W., 2009, Sol Phys., submitted
- Leka, K. D., Fan, Y., & Barnes, G. 2005, ApJ, 626, 1091
- Lionello, R., Velli, M., Einaudi, G., & Mikic, Z. 1998, ApJ, 494, 840
- Liu, Y., Jiang, Y., Haishen, J., Zhang, H., & Wang, H. 2003 ApJ, 593, L137
- Liu, R., Alexander, D., & Gilbert, H. R. 2007, ApJ, 661, 1260

- Liu, R., Gilbert, H. R., Alexander, D., & Su, Y. 2008, *ApJ*, 680, 1508
- Moreno-Insertis, F., & Emonet, T. 1996, *ApJ*, 472, L53
- Sakurai, T. 1976, *PASJ*, 28, 177
- Shimizu, T., et al. 2007, *PASJ*, 59, 845
- Sturrock, P.A. & Woodbury, E.T., 1967, in *Proc. 39th Enrico Fermi School, Plasma Astrophysics*, ed. P. A. Sturrock (New York: Academic), 155
- Tian, L., Bao, S., Zhang, H., & Wang, H. 2001, *A&A*, 374, 294
- Tian, L., Liu, Y. & Wang, J., 2002 *Sol. Phys.*, 209, 361
- Tian, L., Liu, Y., & Wang, H. 2003, *Sol. Phys.*, 215, 281
- Tian, L., Liu, Y., Yang, J., & Alexander, D. 2005, *Sol. Phys.*, 229, 237
- Tian, L., Alexander, D., & Nightingale, R. 2008, *ApJ*, 684, 747
- Tian, L., & Alexander, D. 2009, *ApJ*, 695, 1012
- Titov, V. S., & Démoulin, P. 1999, *A&A*, 351, 707
- Tokman, M., & Bellan, P. M. 2002, *ApJ*, 567, 1202
- Török, T., Kliem, B., & Titov, V. S. 2004, *A&A*, 413, L27
- Török, T., & Kliem, B. 2005, *ApJ*, 630, L97
- Tsuneta, S., et al. 2008, *Sol. Phys.*, 249, 167
- Wang, Y.-M., & Sheeley, N. R., Jr. 1989, *Sol. Phys.*, 124, 81
- Williams, D. R., Török, T., Démoulin, P., van Driel-Gesztelyi, L., & Kliem, B. 2005, *ApJ*, 628, L163

Yan, X. L., & Qu, Z. Q. 2007, *A&A*, 468, 1083

Zaqarashvili, T.V., Chargeishvili, B., & Sakai, J. 1996, *Ap&SS*, 246, 107

Zaqarashvili, T.V., Díaz A., Oliver, R. & Ballester, J.L. 2010, *A&A*(in press)

Zhang, G.-Q., & Tian, L.-R. 2005, *Chinese Journal of Astronomy and Astrophysics*, 5, 77

Zwaan, C. 1985, *Sol. Phys.*, 100, 397

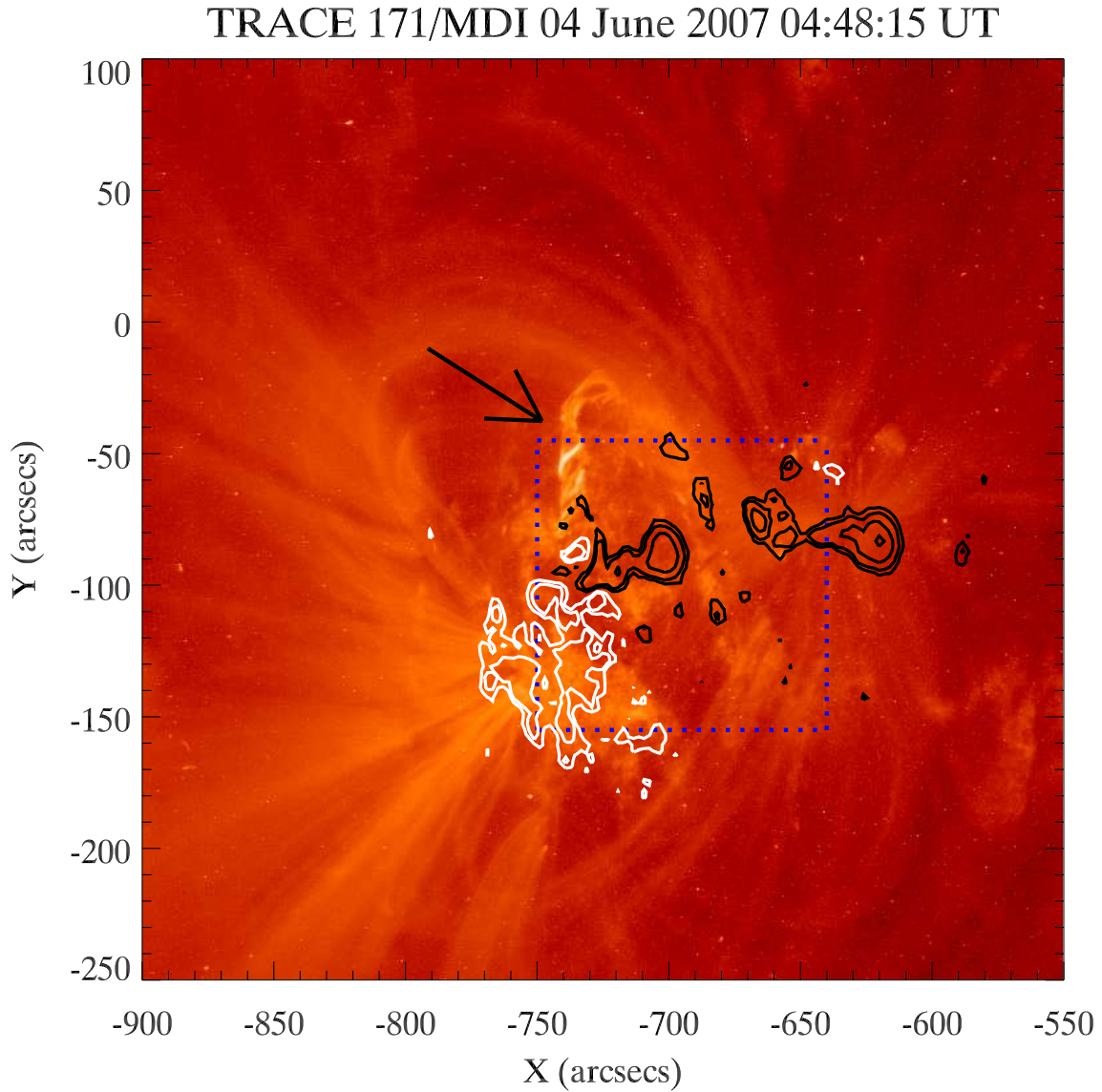


Fig. 1.— Co-aligned MDI contours overlaid on TRACE 171 Å image of the active region AR 10960 on 04:48:15 UT at 4 June, 2007. White (black) contours show the positive (negative) polarity of photospheric magnetic field. The loop with helical twist is shown by the black arrow, while SOT-FOV by blue-dotted square. The left footpoint of the loop is anchored in the small positive polarity spot at $(X,Y)=(-735,-90)$, while the right footpoint is probably anchored in the negative polarity spot at $(X,Y)=(-700,-50)$.

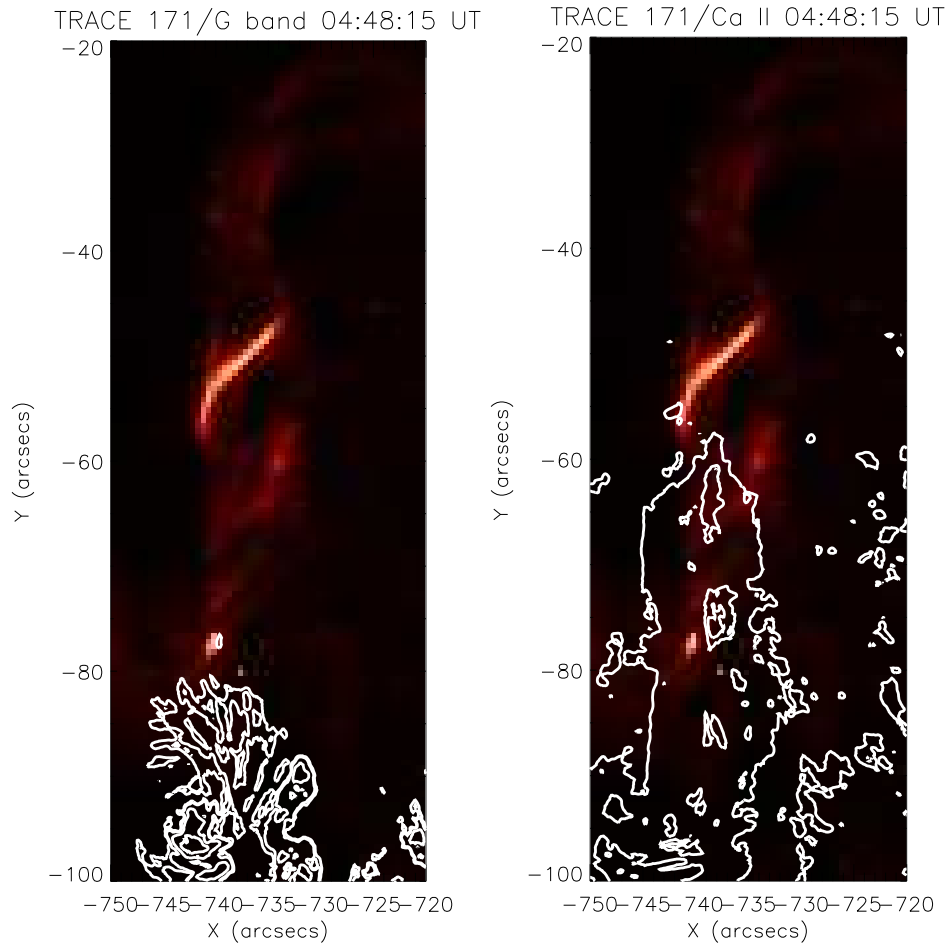


Fig. 2.— Partial FOV of TRACE 171 Å image on 04:48:15 UT at 04 June 2007, which shows the coronal loop segment with strong helical twist. The co-aligned SOT G-band (left panel) and Ca II (right panel) contours are overlaid on TRACE 171 Å image, which show the sunspot position and the chromospheric part of the loop respectively.

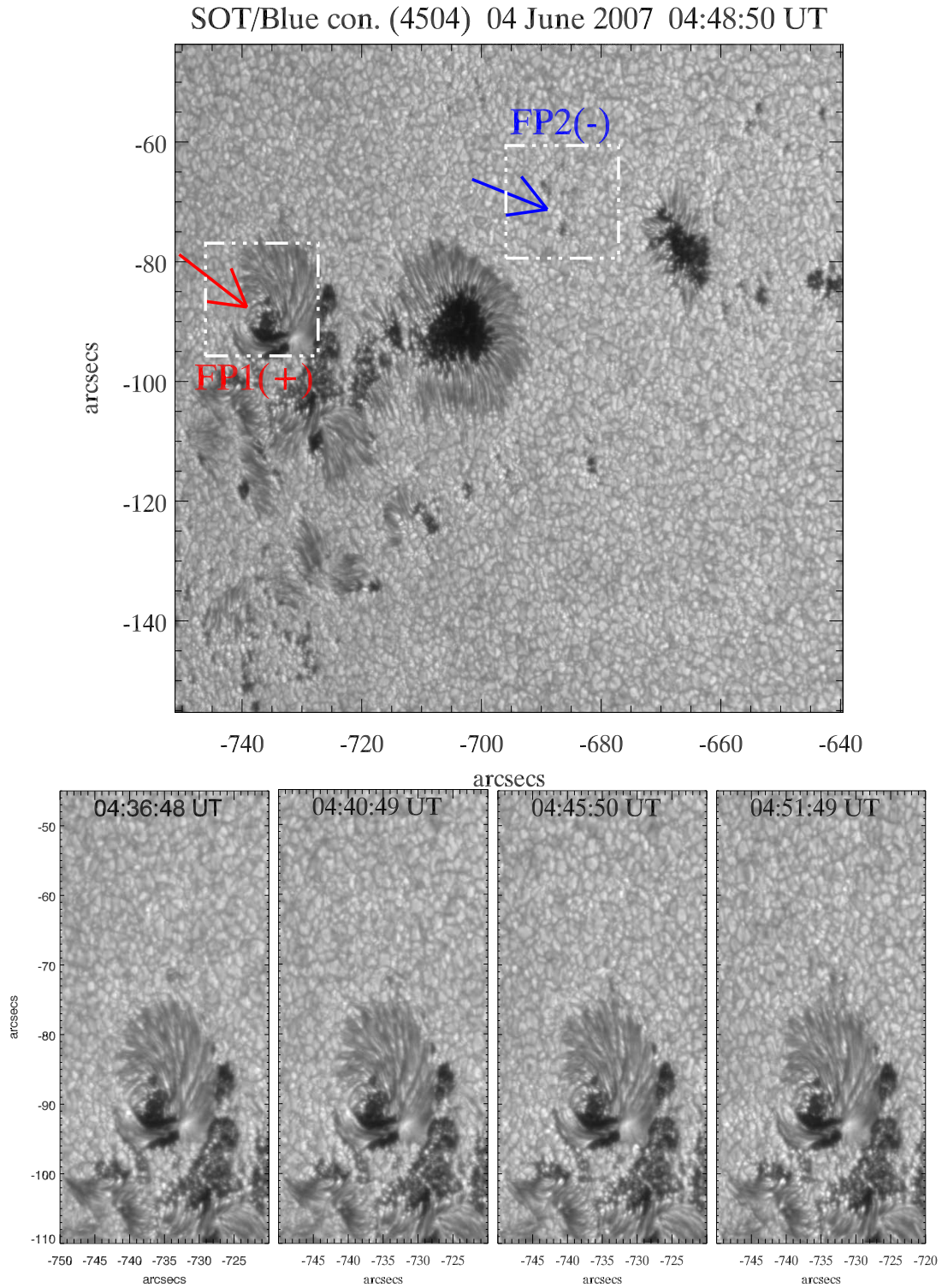


Fig. 3.— The full FOV of AR 10960 in SOT/blue-continuum (4504 \AA) on 04:48:50 UT, which shows the two opposite polarity spots [FP1(+) and FP2(-)] in which respectively the left and right footpoints are anchored (top panel). Partial FOV of AR 10960 in SOT/blue-continuum (4504 \AA) during 04:36 UT and 04:52 UT at 04 June, 2007 at each ~ 3 -4 min interval. The time sequence shows the high-resolution morphology of the spot, where the

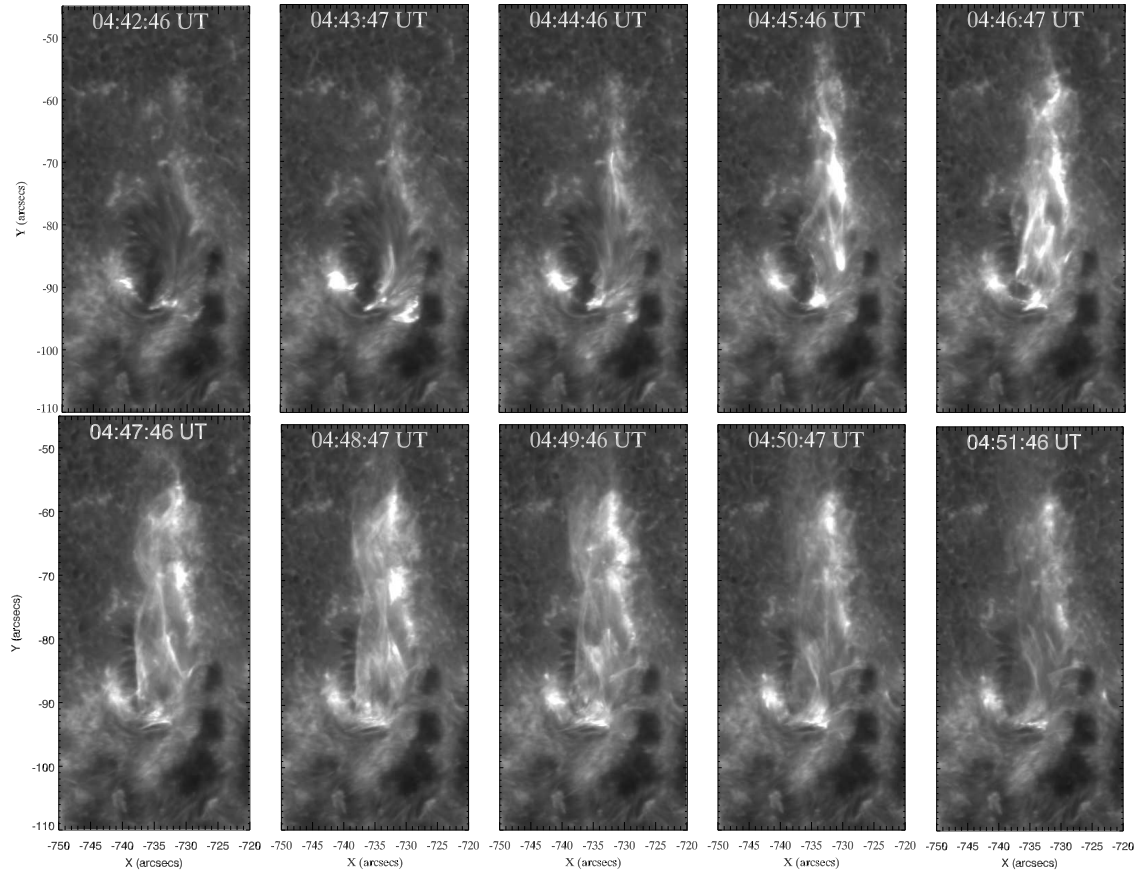


Fig. 4.— Time sequence of SOT/Ca II H (3968 \AA) images during 04:43 UT and 04:52 UT at 04 June, 2007. The images show high-resolution chromospheric morphology of flaring loop. Activation of helical twist and simultaneous brightening in the chromosphere are clearly seen during B5.0 class flare (04:40 UT–04:51 UT).

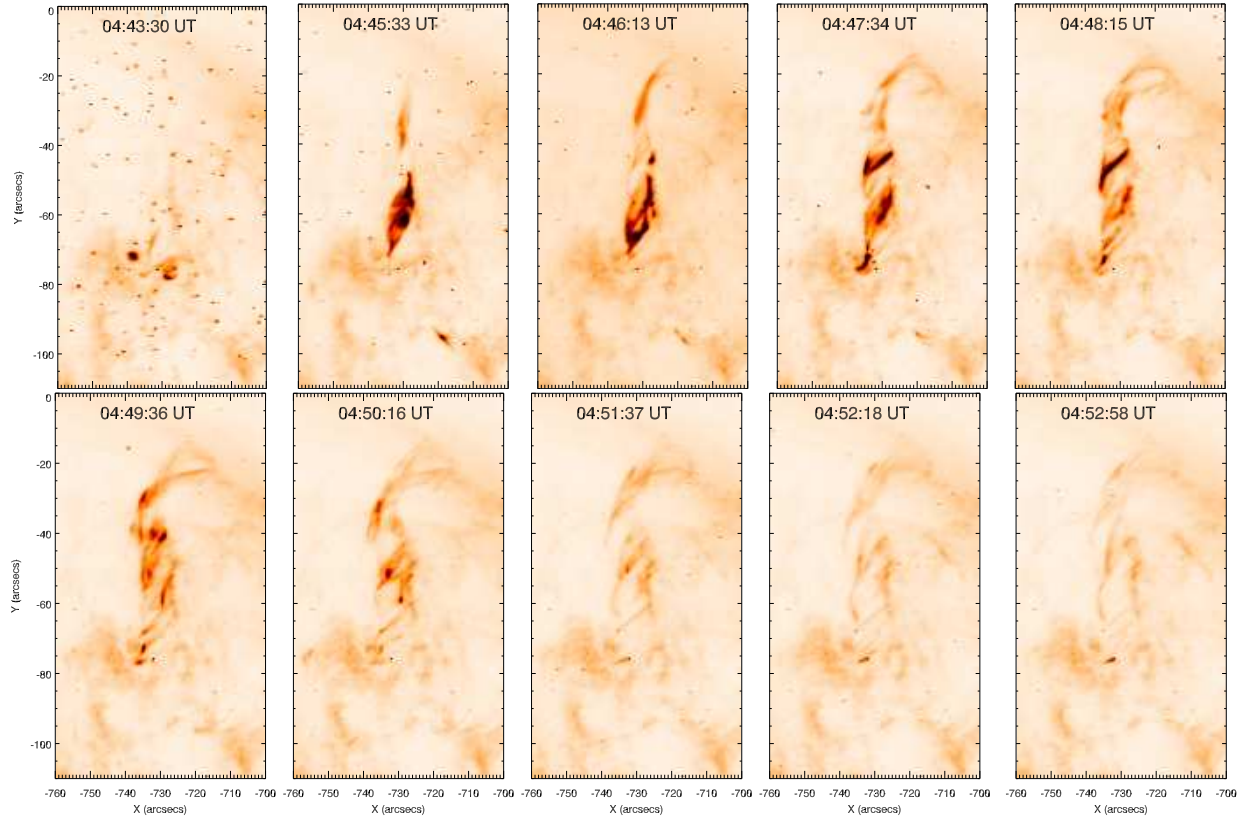


Fig. 5.— Time sequence of TRACE 171 Å Fe IX images of flaring loop in the AR 10960 during 04:43 UT and 04:52 UT on 04 June, 2007. The images are in reverse color and show clear helical twist of the loop during the B5.0 flare. Note the double structure of coronal loop top between 04:47-04:51 UT near $(X,Y)=(-720,-20)$.